

Short-Range Versus Long-Range Order in a Model Binary Alloy*

Michael Plischke and Daniel Mattis

Belfer Graduate School of Science, Yeshiva University, New York, New York 10033

(Received 26 March 1971)

We calculate the free energy of a linear binary metallic alloy using an exact transfer-matrix formalism. We obtain for the first time the electronic band structure when there is nonvanishing short-range order and calculate the temperature dependence of the short-range order parameter. Following Foo and Amar, we also introduce long-range order via two sublattices, but we find this necessarily raises the free energy. We conclude that the first-order phase transition of Foo and Amar is spurious, being an artifact of their assumption of long-range order and neglect of short-range order.

In this Letter we present what we believe to be the first rigorous and self-consistent treatment of the effects of short-range order (SRO) on the electronic density of states of a disordered medium. Recently Foo and Amar¹ reported a surprising first-order phase transition in a simple model of a one-dimensional binary alloy. In this model the atoms do not interact with one another, but contribute to the free energy of the system directly only through their disorder entropy and, indirectly, through the effect of disorder on the electronic density of states. After assuming a variable long-range ordering of the atoms, Foo and Amar calculated the total free energy in the coherent-potential approximation and indeed found a discontinuous disappearance of the sublattice ordering parameter at a finite temperature. The existence of their phase transition would have far-reaching implications for the theory of amorphous materials. For example, it could be the mechanism for a metal-insulator phase transition if a gap in the electronic density of states depended on long-range order.

We disagree with both their procedure and their conclusion. We shall recall Landau's proof² that no matter what long-range order (LRO) we might assume in a linear array, it would "melt" at infinitesimal temperature above absolute zero. Assume an ordered configuration with total free energy F^{LRO} , then break L of the N electronic bonds of the chain at random. This results, on the one hand, in an increased electronic free energy $L|E|$, where E is a temperature-dependent quantity which can be rigorously bounded: $0 < |E| < 1$. This increase is more than compensated by a configurational disorder-related decrease $-kTN[f \ln f + (1-f) \ln(1-f)]$, where $f \equiv L/N$. Minimizing with respect to f , we find that the total free energy is now *lower* than F^{LRO} , thus proving that LRO is thermodynamically unstable. In equi-

librium we find that

$$f = (1 + e^{\beta|E|})^{-1},$$

and the average length \bar{l} of the independent disconnected segments is

$$\bar{l} = f^{-1} - 1 = \exp(\beta|E|)$$

which is finite at any finite temperature. More quantitative arguments are given following Eq. (7).

On the other hand, we compute the short-range order parameter, and find it to be a smooth function of the temperature (see Fig. 1), vanishing slowly with increasing temperature. This also implies the lack of any significant low-order thermodynamic phase transition within the accuracy of our calculation, as well as the absence of LRO in this model. Finally, we obtain the elec-

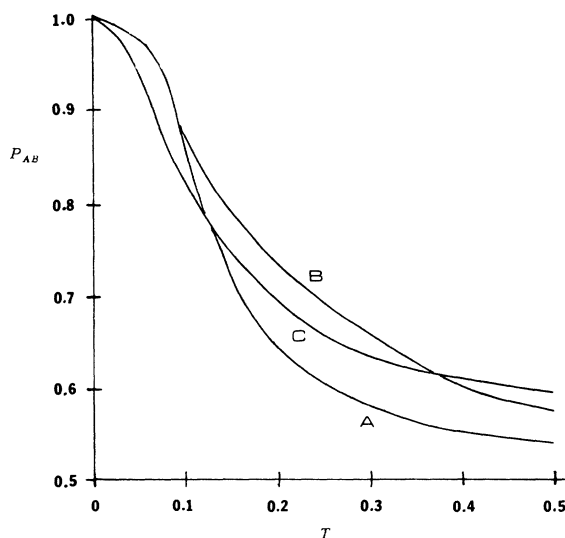


FIG. 1. Plot of SRO parameter $P_{AB}(T)$ as function of T . A, $\epsilon=1.0$; B, $\epsilon=2.0$; and C, $\epsilon=3.0$. At low temperatures curve B is almost indistinguishable from curve A.

tronic density of states and study the energy gap as a function of temperature.

Let us consider the same infinite one-dimensional chain as in Ref. 1, with "hopping" parameter set equal to unity:

$$H = \sum_i |i\rangle \epsilon_i \langle i| - \sum_{i,j=i\pm 1} |i\rangle \langle j|. \quad (1)$$

Here $\epsilon_i = \epsilon_A$ or ϵ_B . We assume an equal number of A and B atoms and without loss of generality adjust the zero of energy such that $\epsilon_A = -\epsilon_B = \epsilon$. In the case of SRO one introduces the parameter P_{AB} , defined to be the probability that an A atom on the n th site has a B atom as its right-hand neighbor. By left-right symmetry $P_{AB} = P_{BA}$. Also $P_{AA} \equiv 1 - P_{AB} = P_{BB}$. To compute the electronic density of states we use the exact formalism of Schmidt.³ The integrated density of states, $M(\omega) = \int_{-\infty}^{\omega} d\omega' \rho(\omega')$, may be obtained from the following equations:

$$M(\omega) = -\frac{1}{2} [W_A(\omega, -\pi) + W_B(\omega, -\pi)], \quad (2)$$

where W_A and W_B obey the equations

$$\begin{aligned} W_A(\omega, \varphi) &= P_{AA} W_A(\omega, T_A \varphi) + P_{AB} W_B(\omega, T_B \varphi) \\ &\quad - P_{AA} W_A(\omega, -\pi) - P_{AB} W_B(\omega, -\pi), \\ W_B(\omega, \varphi) &= P_{BA} W_A(\omega, T_A \varphi) + P_{BB} W_B(\omega, T_B \varphi) \\ &\quad - P_{BA} W_A(\omega, -\pi) - P_{BB} W_B(\omega, -\pi), \end{aligned} \quad (3)$$

with the conditions

$$\begin{aligned} W_j(\omega, \varphi + 2\pi) &= W_j(\omega, \varphi) + 1, \\ W_j(\omega, 0) &= 0, \quad j = A, B, \end{aligned} \quad (4)$$

and where $W_j(\varphi)$ is monotonically increasing; also,

$$T_j \varphi \equiv 2 \tan^{-1}(\epsilon_j - \omega - \cot \frac{1}{2} \varphi). \quad (5)$$

We obtain $W_A(\omega, \varphi)$, $W_B(\omega, \varphi)$ by dividing the interval $0 \leq \varphi \leq 2\pi$ into N subintervals. By linear interpolation over a subinterval we obtain $N-1$ linear equations. It has been shown by Agacy³ that while this procedure does not converge very well to give the density of states, $\rho(\omega) = dM(\omega)/d\omega$, it nevertheless does yield the integrated density of states accurately even for choices of N as low as 20. The electronic free energy in the case of a half-filled band, including the entropy of the electrons, can be expressed in terms of $M(\omega)$ by a partial integration:

$$\begin{aligned} F_{e1}(T, P_{AB}) &= -kT \int_{-\infty}^{\infty} d\omega \rho(\omega) \ln(e^{-\beta\omega} + 1) \\ &= \int_{-\infty}^{\infty} d\omega M(\omega) (e^{\beta\omega} + 1)^{-1}. \end{aligned} \quad (6)$$

We estimate that F_{e1} obtained from $M(\omega)$ calculated for $N = 60$ is correct to within 0.1% at all

temperatures by comparison with spot checks using $N = 120$ and $N = 240$. In one dimension, the configurational atomic entropy associated with SRO parameter P_{AB} has the simple expression

$$\begin{aligned} S(P_{AB}) \\ = -k [P_{AB} \ln P_{AB} + (1 - P_{AB}) \ln(1 - P_{AB})]. \end{aligned} \quad (7)$$

We now wish to buttress the general arguments against LRO in one dimension by a *quantitative* calculation of the extra energy required to introduce LRO, the results of which are given in Fig. 2. For definiteness, we consider precisely the two-sublattice model of LRO defined in Ref. 1. As it happens, the identical formula (7) also obtains for LRO if one suitably redefines P_{AB} to represent the probability of finding a B atom on an A -sublattice site (or an A atom on the B sublattice) and allows $P_{AA} = P_{BB}$ to stand for the probability of finding an atom on its proper sublattice. Once we have the equation suitable for determining W in this case, we can find $M(\omega)$ appropriate to LRO and obtain an exact⁴ expression for F_{e1}^{LRO} using Eq. (6). The appropriate equations for W^{LRO} are

$$\begin{aligned} W_A(\omega, \varphi) &= P_{AA} W_B(\omega, T_B \varphi) \\ &\quad + (1 - P_{AA}) W_B(\omega, T_A \varphi) - W_B(\omega, -\pi), \\ W_B(\omega, \varphi) &= P_{AA} W_A(\omega, T_A \varphi) \\ &\quad + (1 - P_{AA}) W_A(\omega, T_B \varphi) - W_A(\omega, -\pi), \end{aligned} \quad (8)$$

where W_A and W_B obey the same conditions (4) and T_j is again defined by (5). We numerically calculate F^{LRO} (not shown here), and compare it

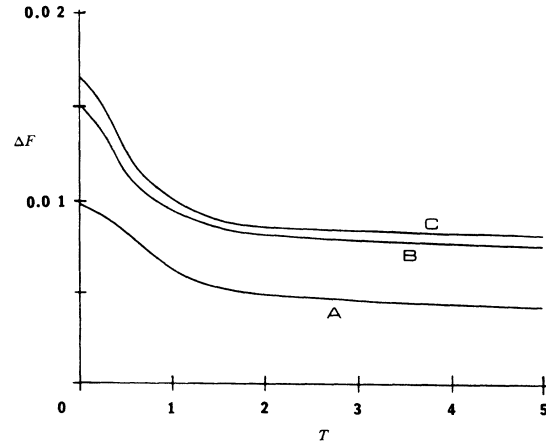


FIG. 2. Plot of $\Delta F = F_{e1}^{\text{LRO}} - F_{e1}^{\text{SRO}}$ as function of T for some typical fixed values of P_{AB} at $\epsilon = 1$. A, $P_{AB} = 0.6$; B, $P_{AB} = 0.7$; and C, $P_{AB} = 0.8$. At $P_{AB} = 1$ (perfect LRO) and $P_{AB} = 0.5$ (disorder) $\Delta F = 0$.

with F^{SRO} . In Fig. 2 the differences in electronic free energies $F_{\text{el}}^{\text{SRO}}$ and $F_{\text{el}}^{\text{LRO}}$ are shown as functions of temperature for various P_{AA} . As seen in this figure, we find $F_{\text{el}}^{\text{SRO}} < F_{\text{el}}^{\text{LRO}}$ at the same value of P_{AA} . It immediately follows that at any temperature T the total free energies obey the relation $F^{\text{SRO}}(T) < F^{\text{LRO}}(T)$, where $F \equiv F_{\text{el}} - TS$. For, suppose that we have obtained the stationary LRO state by minimizing F^{LRO} with respect to P_{AA} . At the value of P_{AA} for which F^{LRO} has a minimum, $F^{\text{SRO}}(P_{AA}, T) < F^{\text{LRO}}(P_{AA}, T)$. But F^{SRO} is not yet at its own minimum and can be further minimized. Thus SRO is, by a finite margin, more stable than LRO. (The possibility that yet other forms of LRO, not considered by Foo and Amar or by us, such as $AABB\cdots$, etc., might be more stable than SRO has already been discounted by the Landau-type arguments offered at the beginning of this paper.)

From the minimization of $F^{\text{SRO}}(T)$ we obtain the equilibrium free energy and the SRO parameter $P_{AB}(T)$ which is plotted in Fig. 1 for $\epsilon = 1, 2, 3$. In all cases, $P_{AB}(T)$, together with the free energy and its various derivatives, varies smoothly with temperature, supporting the conclusion that there is no phase transition in this system. The first-order phase transition of Foo and Amar is an artifact of their assumption of LRO.

One of our calculated results is the differential density of states, $\rho(\omega, P_{AB})$. As has been shown by Agacy³ it is an extremely "noisy" function. The following features, however, are clear: At $P_{AB} = 1$ (perfect LRO) $\rho(\omega)$ has a gap of width 2ϵ centered about $\omega = 0$. For $P_{AB} < 1$, states appear in the gap and begin to fill it up. We arbitrarily define a temperature-dependent "gap" $\Delta(P_{AB})$ as twice the distance between $\omega = 0$ and the point ϵ_c at which the density of states exceeds the "round-off error noise," $\rho(\epsilon_c) \geq 10^{-3}$. In Fig. 3 we plot $\Delta/2\epsilon$ as function of P_{AB} for $\epsilon = 1, 2, 3$. With the use of Fig. 1 for P_{AB} as a function of T , this yields $\Delta(T)$. For $\epsilon = 3$ some gap remains even at total disorder, in accord with the Saxon-Hutner theorem, whereas at $\epsilon = 2$ and 1 the gap disappears before total disorder ($P_{AB} = 0.5$ or $T = \infty$) is reached. We find the slope $d\Delta(T)/dT$ to be discontinuous at the point where the gap vanishes (see curves A and B). On the other hand, we see no discontinuity in any other thermodynamic variables we have calculated, and in one dimension we do not expect any. Therefore, we can only conclude that, within the accuracy of our calculation, and for reasons we do not yet fully grasp, the gap may not be chosen as a proper thermody-

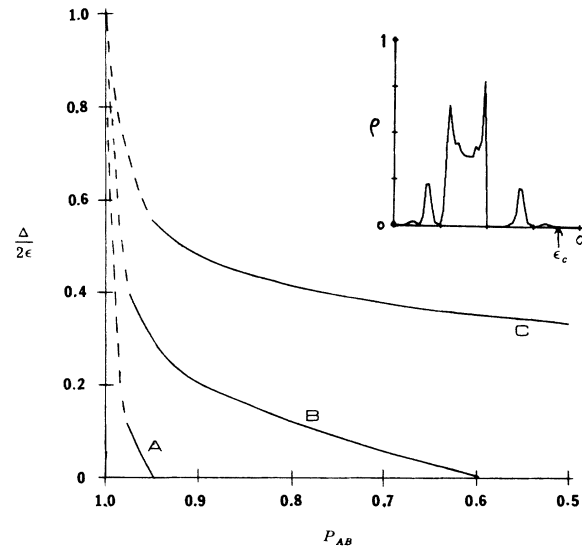


FIG. 3. Plot of the gap parameter $\Delta(P_{AB})/2\epsilon$ as function of $P_{AB}(T)$. A, $\epsilon = 1$; B, $\epsilon = 2$; and C, $\epsilon = 3$. Those parts of the curves which we have extrapolated, but not computed, are indicated by dashed lines. Insert shows a typical density of states, for $\epsilon = 2$ and $P_{AB} = 0.9$, for $\omega > 0$, $\rho(\omega) = \rho(-\omega)$.

namic variable. The question of a metal-insulator transition is left open as it is possible that some, or all, of the states are localized, regardless of whether or not a gap exists.

In conclusion we would like to draw attention to the crossing of the curves in Fig. 1. This seems to indicate that this model cannot be approximated by an Ising model with a temperature-independent coupling constant, and thus casts doubts on the traditional Bragg-Williams approach to the structure of binary alloys.

We thank Dr. J. E. Gubernatis and Professor Philip L. Taylor for a very useful comment³ on the computation of solutions to Eq. (2)-(5).

*Research sponsored by the U. S. Air Force Office of Scientific Research, Air Force Systems Command, under Grant No. AFOSR-69-1642.

¹E.-N. Foo and H. Amar, Phys. Rev. Lett. **25**, 1748 (1970).

²L. Landau and E. Lifschitz, in *Statistical Physics* (Oxford U. Press, Oxford, 1938), p. 232.

³H. Schmidt, Phys. Rev. **105**, 425 (1957). This, as well as R. L. Agacy, Proc. Phys. Soc., London **83**, 591 (1964), is reprinted in *Mathematical Physics in One Dimension: Exactly Soluble Models of Interacting Particles*, edited by E. H. Lieb and D. C. Mattis (Academic, New York, 1966). See also the more recent work of B. Y. Tong, Phys. Rev. **175**, 710 (1968). In the application of these methods, a relaxation method as suggested to us by Gubernatis and Taylor (private commu-

nication) converges very fast without requiring vast computer storage. This allows one to set N as large as 10^3 without much effort, and allowed us to obtain quite satisfactory accuracy in the final results, as discussed in the text.

⁴The methods used in Ref. 1 might be criticized on account of the several approximations (such as the use

of the coherent-potential approximation, and approximating F_{el} by the electronic internal energy with neglect of the electronic entropy). The free energy we calculate, on the other hand (denoted F^{LRO}), is exact within the postulates of the model and free of any approximations except those which arise in numerical computation.

Symmetric Fission Observed in Thermal-Neutron-Induced and Spontaneous Fission of $^{257}\text{Fm}^\dagger$

W. John, E. K. Hulet, R. W. Lougheed, and J. J. Wesolowski

Lawrence Radiation Laboratory, University of California, Livermore, California 94550

(Received 14 May 1971)

The observed mass distribution for thermal-neutron-induced fission of ^{257}Fm is strongly symmetric, whereas that for spontaneous fission of ^{257}Fm is found to be predominantly asymmetric with, however, some symmetric fission present. The mass distributions were derived from energy measurements on coincident fission fragments. The onset of symmetric fission at ^{257}Fm supports theories relating asymmetric fission to the second hump of the fission barrier.

The understanding of the mass distribution in nuclear fission is an outstanding problem. The simple liquid-drop model predicts symmetric fission, yet mass distributions observed for low-energy fission have always been asymmetric. Our measurements on the thermal-neutron-induced fission of ^{257}Fm show a strong mode of symmetric fission. We also observe the symmetric-fission mode occurring weakly in the spontaneous fission of ^{257}Fm , in agreement with the recent data of Balagna *et al.*¹ These unusual results afford an additional test of theories of the mass distribution in fission and, indeed, support a recent suggestion by Möller and Nilsson² relating the mass distribution to the double-humped fission barrier.

Measurements were made on the kinetic energies of the coincident fission fragments from a thin sample placed between two Si detectors. The sample, containing 4×10^8 atoms of ^{257}Fm , was obtained from the Hutch underground nuclear explosion.³ α emission is the predominant decay mode of this 100-day isotope although a small (0.2%) spontaneous-fission branching also occurs. After final purification, a few microliters of solution containing ^{257}Fm was evaporated on a 200- $\mu\text{g}/\text{cm}^2$ Pt foil. The foil was then mounted on a four-position sample wheel located between the two Si detectors with collimators to limit the maximum fragment entry angle to 50° from the normal to the detectors. Other positions of

the wheel contained a ^{252}Cf spontaneous-fission source for energy calibration, a ^{235}U source (2 ng) for neutron-flux determination and a check on the energy calibration, and a blank Pt foil for background measurement. All samples were covered by 200- $\mu\text{g}/\text{cm}^2$ Pt foils to prevent detector contamination. The assembly was placed in the thermal column of the Livermore reactor in a flux of 2×10^{11} neutrons/ cm^2 sec (cadmium ratio 600). The techniques for counting in the high neutron flux included cooling the detectors and using fast linear electronics as previously described.⁴ Data were accumulated alternately with the reactor on and then off. Two separate runs of about three weeks each were made. The fragment masses for each event were calculated from the kinetic energies, assuming conservation of momentum and mass. A correction was made for the pulse-height defect but not for neutron emission. Thus the masses correspond to provisional (approximate pre-neutron) masses of Schmitt, Neiler, and Walter.⁵

In Fig. 1 the results for spontaneous fission of ^{257}Fm are displayed as a contour diagram of counts versus fragment mass and total kinetic energy. The symmetric part of the distribution is evident as a ridge along the line of mass symmetry extending up to 250 MeV. The greatest number of events occurred on the asymmetric peaks at masses 115 and 142 with a total post-neutron kinetic energy of 188 MeV. A graph of